Identification and Compensation of Gyroscope Measurement Errors: Signal Filtering Based on Static and Dynamic Measurements in an Inertial Navigation System

Szymon Elert
Military Institute of Armament Technology, ul. Wyszyńskiego, 05-220 Zielonka, Poland

Abstract: This paper addresses the issue of identifying measurement errors in the MEMS gyroscope, which serves as the primary source of data for the rocket's inertial navigation system (INS). The research focused on error analysis through static and dynamic testing, followed by a detailed analysis of angular velocity measurement data from the flight of a stabilized rocket, guided to a specific point in space. The objective of the study was to determine and filter gyroscope measurement errors, such as bias, random walk, and noise. An adaptive filter was proposed, which adjusts to the changing dynamics of the rocket, allowing for more effective compensation of these errors. In the final section, conclusions are presented that identified shortcomings in the algorithm and outlined directions for further work on its optimization. The algorithm was validated in static, dynamic, and actual rocket flight conditions.

Keywords: measurement error compensation, MEMS gyroscope, adaptive filtering, inertial navigation, missile navigation systems

1. Introduction

Gyroscopes play a critical role in inertial navigation systems (INS), which are widely used in aerospace applications, including the navigation systems of rockets. As the primary sensor responsible for measuring angular velocity, gyroscopes provide essential data that is used to estimate the orientation and movement of a vehicle. In the context of rocket navigation, the accuracy and reliability of gyroscopes are paramount, as even small measurement errors can lead to significant deviations in trajectory or instability during flight [1–3]. Inertial navigation systems are autonomous systems that calculate position, velocity, and orientation based solely on data from internal sensors, such as gyroscopes and accelerometers. Unlike GPS, which relies on external satellite signals, INS operates independently, making it highly useful in environments where external signals are unavailable or unreliable, such as during rocket flights through the atmosphere or in space. This autonomy provides a significant advantage in aerospace applications, particularly in terms of system robustness and reliability.

Autor korespondujący:
Szymon Elert, elerts@witu.mil.pl

Artykuł recenzowany
nadesłany 10.04.2025 r., przyjęty do druku 22.07.2025 r.

However, INS also presents several challenges, particularly related to the accumulation of errors over time. Gyroscope measurements, while generally accurate in the short term, are susceptible to drift, bias, and noise. These errors, if not properly managed, can lead to increasing inaccuracies in the estimated position and orientation of the rocket. To mitigate these issues, advanced filtering algorithms, such as the Kalman filter, are employed to improve the accuracy of sensor data by compensating for known error sources. There have been numerous studies on compensating for gyroscope errors, ranging from simple methods such as Moving Average Filters [4], to advanced techniques utilizing neural networks [5–7]. For a long time, the Kalman filter has been a proven and widely used method, extensively described in the literature [8–14, 32]. Since this filter cannot always be directly applied to nonlinear models, it has been modified to increase its flexibility by dynamically adjusting the parameters of the covariance matrices Q and R, al-lowing for more effective filtering in systems with variable dynamics [15,16]. Stochastic processes are also increasingly employed, as they enable the identification of errors in gyroscopes, such as nonlinear bias and measurement noise, which are difficult to eliminate. The results of these studies have been presented in the literature [17,18]. Available research also shows results focusing on the elimination of specific stochastic errors, such as Allan variance analysis [19–21], quantum random walk [22], or Gaussian Noise [23].

One of the promising solutions is the application of advanced signal decomposition methods, such as improved

Empirical Mode Decomposition (EMD) combined with the ARMA model. Zeng et al. [24] demonstrated that this approach effectively separates and compensates for random errors in MEMS gyroscopes, reducing the root mean square (RMS) error by more than 50 % in both static and dynamic tests. Another important area of research is the real-time compensation of temperature-related errors, which significantly affect the accuracy of MEMS gyroscopes in aerospace environments. Wang et al. [25] developed an automatic demodulation phase error compensation algorithm that ensures stable gyroscope performance across a wide temperature range (from –40 °C to +60 °C), improving bias stability to levels below 0.1 °C/h. In the field of artificial intelligence, Shen et al. [26] combined Long Short-Term Memory (LSTM) neural networks with the Kalman filter and the Expectation-Maximization (EM) algorithm to compensate for bias drift in environments with random vibrations. This method demonstrated high effectiveness in dynamic testing conditions, confirming the potential of machine learning in modeling complex, time-varying measurement errors. Recent publications also describe the use of ensemble learning algorithms, such as XGBoost and Multi-Layer Perceptron (MLP) neural networks, for automatic calibration of MEMS gyroscopes [27]. Additionally, the new MoE-Gyro framework, based on Mixture of Experts networks, enables simultaneous signal reconstruction beyond the measurement range and noise reduction, significantly extending the dynamic range and improving the noise characteristics of MEMS gyroscopes [28].

The use of gyroscopes in rocket navigation offers both advantages and limitations. On the one hand, INS provides continuous, real-time updates on the vehicle's state without relying on external data sources, which is crucial for maintaining control and stability throughout the mission. On the other hand, the inherent errors in gyroscope measurements require sophisticated error identification and compensation techniques to ensure the system's performance meets the stringent requirements of aerospace navigation. This paper focuses on the identification of gyroscope measurement errors and the implementation of signal filtering techniques based on both static and dynamic measurements. By analyzing these errors and applying appropriate compensation methods, it is possible to improve the overall accuracy and reliability of inertial navigation systems (INS) in rocket applications, ensuring precise navigation and control throughout the mission. In the proposed approach, adaptation was implemented by dynamically adjusting the parameters of the Kalman filter according to the current flight conditions of the rocket. A key element of this adaptation involved modifying the process noise variance matrix (Q) based on the increments of angular velocity measured by the gyroscope. During highly dynamic phases of flight, characterized by large changes in angular velocity, the filter reduced its reliance on the theoretical model and increased the weight of the current measurements, allowing for a faster response to changing flight conditions. Conversely, during stable flight phases, where angular velocity changes were minimal, the filter relied more on the motion model, reducing the influence of measurement noise. This approach allowed the filter to flexibly adapt its operation, ensuring high estimation accuracy under both dynamic and static conditions.

2. Mathematical model of gyroscope

2.1. Measurement model description

The rocket navigation system is based on various, often integrated systems such as the Inertial Navigation System, the Global Navigation Satellite System (GNSS), and the Astronavigation System. This study focuses on the analysis of measurement data from the Inertial Measurement Unit (IMU), whose measurements provide real-time navigation data estimates for the rocket. The IMU used in the research is built using MEMS technology, with its specific parameters listed in Table 1. This unit contains two orthogonal triads of sensors: one consisting of accelerometers and the other of gyroscopes. The accelerometers measure linear motion in three directions, while the gyroscopes measure angular motion in three directions. In addition to inertial sensors, the unit also includes electronics that enable preliminary data filtering and provide measurement output via digital signals

Tab. 1. Basic parameters of the inertial navigation unit used in the research
Tab. 1. Parametry jednostki nawigacji inercyjnej wykorzystanej do badań

Parameter	Value
Angular random walk (deg/√h)	0.15
Bandwidth (Hz)	131
Bias Instability (deg/h)	0.5
Orthogonality (mrad)	0.2
Scale factor (ppm)	500

Due to the focus of this study on the analysis of errors and the correction of measured angular velocities, the mathematical model of the gyroscope is presented below in the form of the observation equation for angular velocity measurements [12], which accounts for key errors affecting measurement accuracy. This model serves as the fundamental basis for analyzing and correcting angular velocity measurement errors, which are critical in navigation systems, such as INS.

$$\tilde{\omega}_b = S \cdot N \cdot \omega_b + b_g + \varepsilon_g, \tag{1}$$

where: $\tilde{\omega}_b$ – gyroscope measurement vector (deg/s), ω_b – true angular rate velocity vector (deg/s), b_g – gyroscope instrument bias vector (deg/h), S – matrix representing the gyro scale factor, N – vector representing non-orthogonality of the gyro triad, ε_g – vector representing the gyro sensor noise (deg/h).

2.2. Mathematical errors description

The measurement of angular velocities from the gyroscope actually consists of various types of errors, which affect the measured values to a greater or lesser extent. Their occurrence depends on the dynamics of the measured object and the environment in which the measurements are performed. Due to their origin, several main types of errors are distinguished, which were taken into account during the tests:

— Bias is a systematic error whose value remains constant over a short period of time but may slowly change over a longer period. In the case of long-term measurements, bias can gradually shift, leading to an accumulating error in the measurements. However, within shorter time intervals, its value is generally stable, causing a consistent offset in the measurement results. It is a systematic error that does not change within a specific time frame, but during longer measurements, its value may experience slight increases. Therefore, the equation for bias in discrete form, ac-counting for slow change over time, i.e., drift, is presented below:

$$b_g[k] = b_2[k]^2 + b_1[k] + b_0, \tag{2}$$

where: $b_g[k]$ – value of bias at the discrete time step k, k – discrete value of the bias at time $t_k = k \cdot \Delta t$, Δt – time between next measurements, b_2 – polynomial coefficient 2nd

order, b_1 – polynomial coefficient 1st order (linear drift), b_0 – initial value drift.

– The scale factor is the deviation of the input-to-output gradient from unity, and it is therefore proportional to the actual angular velocity around the gyroscope's sensitivity axis [12]. Inaccuracies in the gyroscope's scale factor affect the accuracy of the angular velocity measurement. Typically, the IMU manufacturer provides information about the scale factor value in the documentation; however, to obtain an accurate scale factor, an analysis of this parameter was conducted based on the static testing of the sensor. The values provided by the manufacturer are usually given in units of ppm, which means parts per million.

$$SF = 1 + \frac{SF_{acc}}{10^6}, \tag{3}$$

where: SF – scale factor, SF_{acc} – scale factor defined by manufacturer (accuracy).

Determination SF_{acc} empiric method:

$$SF_{acc} = \frac{\left|SF_m - 1\right|}{1} \cdot 10^6, \tag{4}$$

where: SF_m – measured scale factor.

$$SF_m = \frac{\mathrm{cov}(\tilde{\omega}_b, \omega_r)}{\mathrm{var}(\omega_r)}, \tag{5}$$

where: $\tilde{\omega}_b$ – gyroscope measurement vector (deg/s), ω_r – gyroscope reference vector (deg/s).

The scale factor values obtained through empirical methods and the scale factor values from the documentation were averaged to obtain the final coefficient S

$$S = \frac{SF_1 + SF_2}{2}, \tag{6}$$

where: SF_1 – gyroscope scale factor form datasheet, SF_2 – gyroscope scale factor calculated form static tests.

– The non-orthogonality error refers to the lack of perpendicularity between the gyroscope's axes. This error causes disturbances in the measurement results for each axis, which in navigation systems can lead to incorrect estimation of the rocket's orientation and trajectory. These errors are identified using specialized devices that rotate the gyroscope around a single axis with high precision, allowing for accurate identification and compensation of the error.
– Sensor noise is a signal that arises from random processes and carries no useful information. This noise significantly affects the accuracy and quality of gyroscope measurements, which can lead to incorrect estimation of orientation angles in space and position. Since it is based on random processes, accurately identifying it is often complicated, especially when the gyroscope is measuring angular velocities of a highly dynamic object, such as a rocket. To properly determine the value of gyroscope noise, all its components must be considered:

Drift – random variation of the gyroscope bias over time. This component is modeled as a random process that gradually accumulates over time and is influenced by other parameters such as temperature.

White noise – random signal with zero mean and a specified standard deviation based on measurements from the gyroscope. This noise is described as a Gaussian process [23, 31].

$$\omega(t) \sim N(0, \sigma^2), \tag{7}$$

where: $\omega(t)$ – gyroscope white noise with zero mean and variance [deg/s].

Random walk (RW) is a parameter that defines the accumulation of measurement errors over time. In a gyroscope, it is caused by bias drift and the presence of white noise. Given that random walk refers to the process by which the angular velocity value changes randomly, its value should be included in the process noise matrix Q in equation (19). The method for determining RW is presented below [33].

$$RW = \mathrm{var}(\Delta\omega), \tag{8}$$

where: RW – variance of the accumulation of measurement errors over time [deg/s^2], $\Delta\omega$ – difference in the increments of angular velocities [deg/s].

$$\Delta\omega = \begin{bmatrix} \Delta\omega_x \\ \Delta\omega_y \\ \Delta\omega_z \end{bmatrix}, \tag{9}$$

$$\Delta\omega_x = \begin{bmatrix} \omega_{bx,2} - \omega_{bx,1} \\ \vdots \\ \omega_{bx,t+1} - \omega_{bx,t} \end{bmatrix}. \tag{10}$$

Quantization Noise (QN) introduces an error into the measured signal resulting from the difference between the analog signal and the nearest digital value at each sampling instant from the quantizer, that is, the analog-to-digital converter. This noise is typically modelled as a stochastic process [30, 31]:

$$q(t) \sim u\left(-\frac{\Delta q}{2}, \frac{\Delta q}{2}\right), \tag{11}$$

where: Δq – difference between two adjacent quantization levels and is expressed by the formula:

$$\Delta q = \frac{\omega_{res}}{2^n}, \tag{12}$$

where: ω_{res} – the total range of the gyroscope's measurement values [deg/s], n – number of bits of the ADC.

Quantization Noise is an important parameter because it can significantly affect the accuracy and quality of results in devices where signals are processed in real-time, such as an inertial navigation unit. This noise has been included in the process noise variance matrix Q in equation (19) as a parameter determined as variance [34, 35]:

$$\mathrm{var}[q(t)] = \frac{\Delta q^2}{12}. \tag{13}$$

2.3. Error determination algorithm

Kalman filtering

Methods for identifying angular velocity measurement errors have been thoroughly described in numerous scientific publications, with selected examples cited in Chapter 1. However, algorithms available in the literature do not always provide satisfactory results under all operational conditions.

The aim of this research was to adjust individual components of the estimation algorithm to minimize the impact of angular velocity measurement errors, which constitute the primary input to the algorithm responsible for determining spatial orientation angles. These orientation angles are subsequently used to calculate the position and velocity of the rocket in the inertial navigation system.

In this study, the Extended Kalman Filter (EKF) was applied as the method for error identification and compensation. The filter was adapted to account for the key sources of errors described in Section 2.2, including drift, random noise, and nonlinear measurement disturbances. EKF was selected as the primary estimation tool due to its ability to simultaneously model the system dynamics and the characteristics of measurement errors in nonlinear state models.

Several key aspects were taken into consideration during the tuning of the algorithm components:

- the rocket exhibits high dynamics; therefore, minimizing algorithmic delays is essential,
- it is necessary to provide measurement data updates as frequently as possible,
- high measurement reliability was ensured by utilizing a test platform simulating rocket motion in three axes (yaw, pitch, roll), allowing for detailed analysis of the obtained results.

The author acknowledges that the EKF is not an optimal estimator for systems with strongly nonlinear state transitions. Therefore, a crucial element of the research was the proper selection of the initial state estimation to ensure reliable filter performance in both static and dynamic tests. The results of these tests are presented in Chapter 3. According to the EKF methodology [12, 16, 32], assuming that ω_b is the actual angular velocity and b_g is the gyroscope bias, the equations were formulated

$$x = \begin{bmatrix} \tilde{\omega}_{bx} \\ \tilde{\omega}_{by} \\ \tilde{\omega}_{bz} \\ b_{gx} \\ b_{gy} \\ b_{gz} \end{bmatrix}. \tag{14}$$

The state transition model for prediction is written as follows:

$$\begin{bmatrix} \tilde{\omega}_b(t+1) \\ b_g(t+1) \end{bmatrix} = \begin{bmatrix} I_3 & 0_3 \\ 0_3 & I_3 \end{bmatrix} \begin{bmatrix} \tilde{\omega}_b(t) \\ b_g(t) \end{bmatrix} + \varepsilon_g. \tag{15}$$

where: I_3 – identity matrix of the measured angular velocities and the gyroscope bias, ε_g – process noise.

Prediction step:

$$x_{pred} = F \cdot x_{est}, \tag{16}$$

where: x_{pred} – the state prediction vector predicting the state before incorporating new measurements, x_{est} – the state estimation vector incorporating measurements and corrections, F – the matrix responsible for the linearization of the nonlinear state transition function.

$$F = \begin{bmatrix} 1 & 0 & 0 & -\Delta t & 0 & 0 \\ 0 & 1 & 0 & 0 & -\Delta t & 0 \\ 0 & 0 & 1 & 0 & 0 & -\Delta t \\ 0 & 0 & 0 & 1 & 0 & 0 \\ 0 & 0 & 0 & 0 & 1 & 0 \\ 0 & 0 & 0 & 0 & 0 & 1 \end{bmatrix}, \tag{17}$$

where: Δt – the sampling time [s].

Prediction error covariance matrix:

$$P_{pred} = F \cdot P_{est} \cdot F^{\mathrm{T}} + Q, \tag{18}$$

where: P_{pred} – prediction error covariance matrix, P_{est} – the estimation of the error covariance matrix determined in the correction step, Q – the process noise variance matrix that accounts for errors such as Random Walk and Quantization Noise and is described as follows:

$$Q = \begin{bmatrix} Q_{\omega,x} & 0 & 0 & -\Delta t & 0 & 0 \\ 0 & Q_{\omega,y} & 0 & 0 & -\Delta t & 0 \\ 0 & 0 & Q_{\omega,z} & 0 & 0 & -\Delta t \\ 0 & 0 & 0 & Q_{b,x} & 0 & 0 \\ 0 & 0 & 0 & 0 & Q_{b,y} & 0 \\ 0 & 0 & 0 & 0 & 0 & Q_{b,z} \end{bmatrix}, \tag{19}$$

where: $Q_{\omega,x}$, $Q_{\omega,y}$, $Q_{\omega,z}$ – the sum of the variance of RW and QN errors, respectively for each axis X, Y, Z; Q_{bx}, $Q_{b,y}$, $Q_{b,z}$ – the representation of the process noise for the bias, respectively for each axis X, Y, Z.

Correction step:

$$K = P_{pred} \cdot H^{\mathrm{T}} \cdot (H \cdot P_{pred} \cdot H^{\mathrm{T}} + R)^{-1}, \tag{20}$$

where: K – Kalman Gain, R – the measurement noise variance matrix for the angular velocities from the gyroscope, H – Jacobian matrix,

$$H = \begin{bmatrix} 1 & 0 & 0 & 1 & 0 & 0 \\ 0 & 1 & 0 & 0 & 1 & 0 \\ 0 & 0 & 1 & 0 & 0 & 1 \end{bmatrix}. \tag{21}$$

Update estimation state:

$$x_{est} = x_{pred} + K \cdot \left(z(t) - H \cdot x_{pred}\right), \tag{22}$$

where: $z(t)$ – the measurement vector that includes the measured angular velocities and the gyroscope bias.

$$z(t) = \begin{bmatrix} \tilde{\omega}_{bx} \\ \tilde{\omega}_{by} \\ \tilde{\omega}_{bz} \\ b_{gx} \\ b_{gy} \\ b_{gz} \end{bmatrix}. \tag{23}$$

Update of the error covariance matrix.

$$P_{est} = (I - K \cdot H) \cdot P_{pred}. \tag{24}$$

Adaptive filtering

To improve the accuracy and flexibility of the algorithm, the Q matrices were multiplied by coefficients whose values depended on the increments of angular velocities measured at each time step. This approach allowed for the dynamic adjustment of the Q matrices according to the current motion conditions, taking into account the changing dynamics of the system. As a result, the Kalman filter responded better to varying flight conditions, significantly enhancing the precision and stability of state estimation in real time.

$$Q_k = a\left(\left|\omega_k - \omega_{k-1}\right|\right) \cdot Q_0, \tag{25}$$

where: Q_k – the process noise variance matrix at step k, ω_k – the measured angular velocity at step k [deg/s], ω_{k-1} – the measured angular velocity at the previous step [deg/s], a – a scaling factor dependent on the increment of angular velocity, Q_0 – is the initial variance matrix.

The correction coefficients a were determined experimentally based on data obtained from the flights of a maneuvering rocket as well as from static and dynamic laboratory tests. A wide range of dynamic conditions was analyzed, including both intense rocket maneuvers in real flight conditions and stable operation phases tested under laboratory conditions.

Based on these studies, optimal values of the coefficients were selected to provide the best possible compromise between the adaptation speed of the filter and the stability of the estimation.

During the operation of the algorithm, the coefficients were not calculated dynamically, but their values were adopted as constant or functionally dependent on the magnitude of the angular velocity increments, in accordance with the results of previous experiments. Their values decreased with increasing increments of angular velocity, leading to a reduction of the process noise in the Kalman filter under dynamic conditions. This allowed the filter to limit the influence of model errors in situations where the dynamic changes in motion provided sufficient information for state estimation, enabling more stable and accurate filtering.

Conversely, in static conditions or during small angular velocity changes, the values of the coefficients increased, leading to an increase in the process noise and, therefore, an increase in the sensitivity of the Kalman filter to minor variations in the signal. This allowed for compensation of modeling errors and uncertainties under low-dynamic conditions.

This approach enabled the Kalman filter to adapt flexibly to changing operating conditions, ensuring high estimation accuracy both during dynamic maneuvers and in stable phases of flight.

3. Results

This chapter presents the results of tests conducted on gyroscopes in three different configurations, aimed at evaluating their performance under static, dynamic, and real rocket flight conditions. The first configuration involved static measurements, which al-lowed for the assessment of basic gyroscope parameters such as drift and inherent noise in ideal conditions, without the influence of motion.

The second configuration included measurements of a gyroscope mounted on a gimbal, simulating the dynamics of rocket flight. This test aimed to replicate real flight conditions in a controlled laboratory environment and enabled the analysis of gyroscope behavior during dynamic maneuvers.

The third configuration was based on real measurements taken during the flight of a subsonic rocket, stabilized in three channels (yaw, pitch, roll), guided to a point in space. This part of the research was crucial for understanding the actual loads and disturbances that gyroscopes are exposed to during flight, which allowed for the assessment of their accuracy and stability in operational conditions.

Below, in Table 2, the values of four coefficients modifying the Q matrix depending on the dynamics are presented.

Tab. 2. Table of dynamic scaling coefficient values applied in the algorithm analysis

Tab. 2. Zestawienie wartości dynamicznych współczynników skali użytych podczas analizy algorytmu

Number of a	Value
a_1	1.05
a_2	0.25
a_3	0.055
a_4	0.0005

The conclusions drawn from the analysis of the results presented in Figure 1 indicate a significant improvement in the quality of angular velocity measurements after applying the proposed filtering algorithm. The algorithm successfully reduced process noise by up to ten times compared to raw data, demonstrating the effectiveness of the adopted filtering approach. Additionally, a correction of gyroscope bias error over time was observed, visible as a gradual convergence of the results toward zero. This means that the algorithm not only reduces noise but also effectively compensates for systematic drift errors, thereby improving measurement accuracy. As a result, the outputs from the proposed algorithm are much closer to actual values, and the improved stability of the gyroscope signal is crucial for further applications in the inertial system.

The conclusions from the analysis of the results presented in Figures 2 and 3, which illustrate angular velocity measurements during the rocket flight simulation with the IMU system mounted on a gimbal, indicate the effectiveness of the applied algorithm in reducing measurement errors. The algorithm performs well in eliminating noise that obscured the signal, allowing

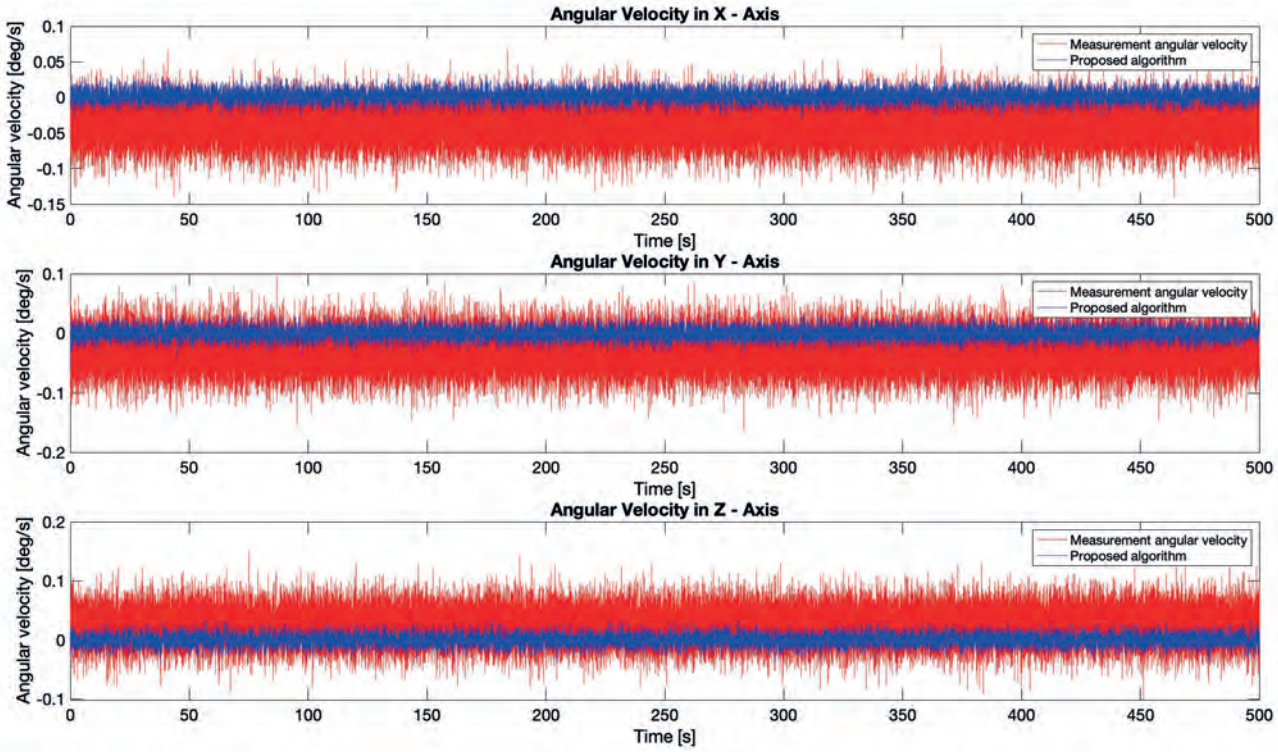

Fig. 1. Comparison of the measured angular velocity signals from gyroscopes with the filtered signals in the static test
Rys. 1. Porównanie sygnałów zmierzonych prędkości kątowych z giroskopów z sygnałami przefiltrowanymi w badaniu statycznym

for clearer and more reliable data regarding flight dynamics. However, some delay in measurement responses can be observed on the charts, which is due to the low sampling frequency of the IMU, set at 250 Hz in this case. Despite this limitation, the algorithm still provides significant signal quality improvement, which is important for further analysis of rocket dynamics and precise reproduction of its movement. However, a higher sampling frequency could minimize delays and further improve measurement accuracy.

Furthermore, Figure 3 presents selected segments of the measured angular velocity signals for each axis. These segments clearly show the smoothing of the measurement signals from the gyroscopes. This effect results from the reduction of noise generated by the sensor, which significantly improves the clarity and stability of the signal in the analyzed measurement ranges. Figure 5 presents data recorded during the flight of a subsonic rocket, stabilized in three channels and guided to a specific point in space. The chart shows varying effectiveness of the algorithm

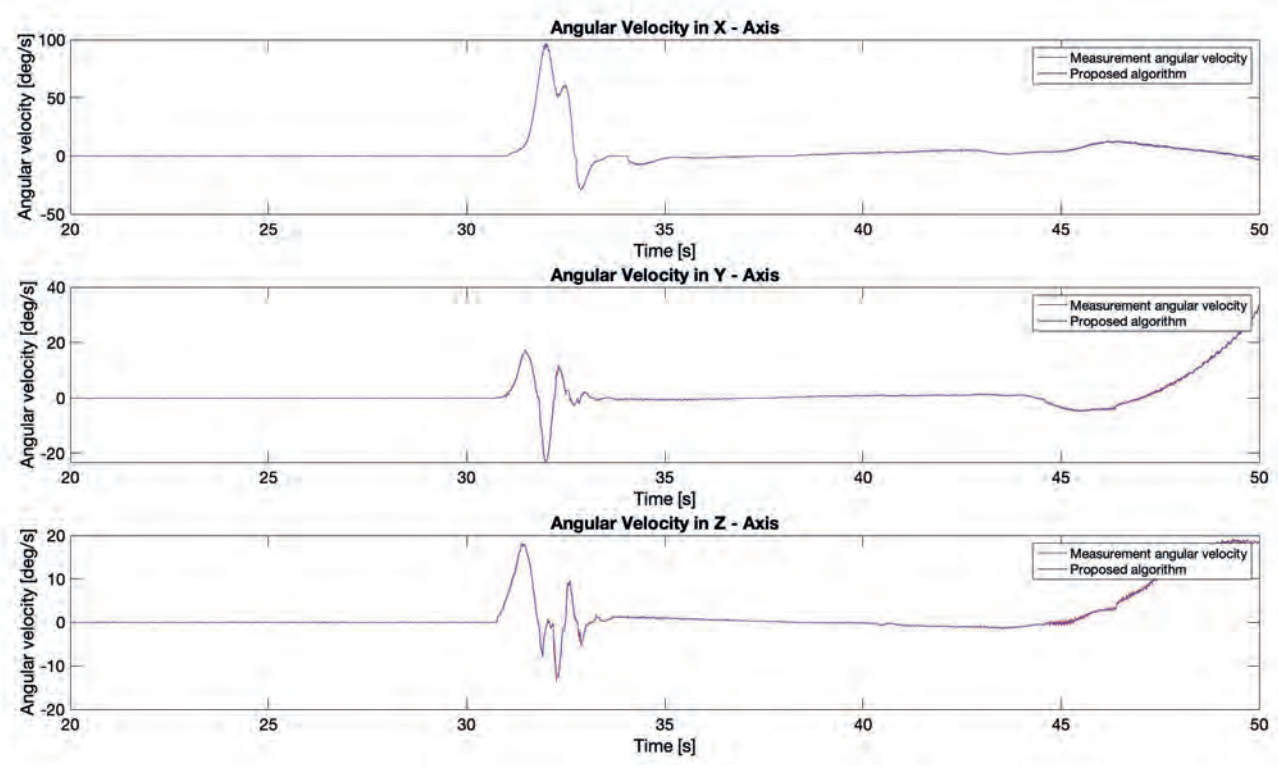

Fig. 2. Comparison of the measured angular velocity signals from gyroscopes with the filtered signals in the dynamic test
Rys. 2. Porównanie sygnałów zmierzonych prędkości kątowych z giroskopów z sygnałami przefiltrowanymi w badaniu dynamicznym

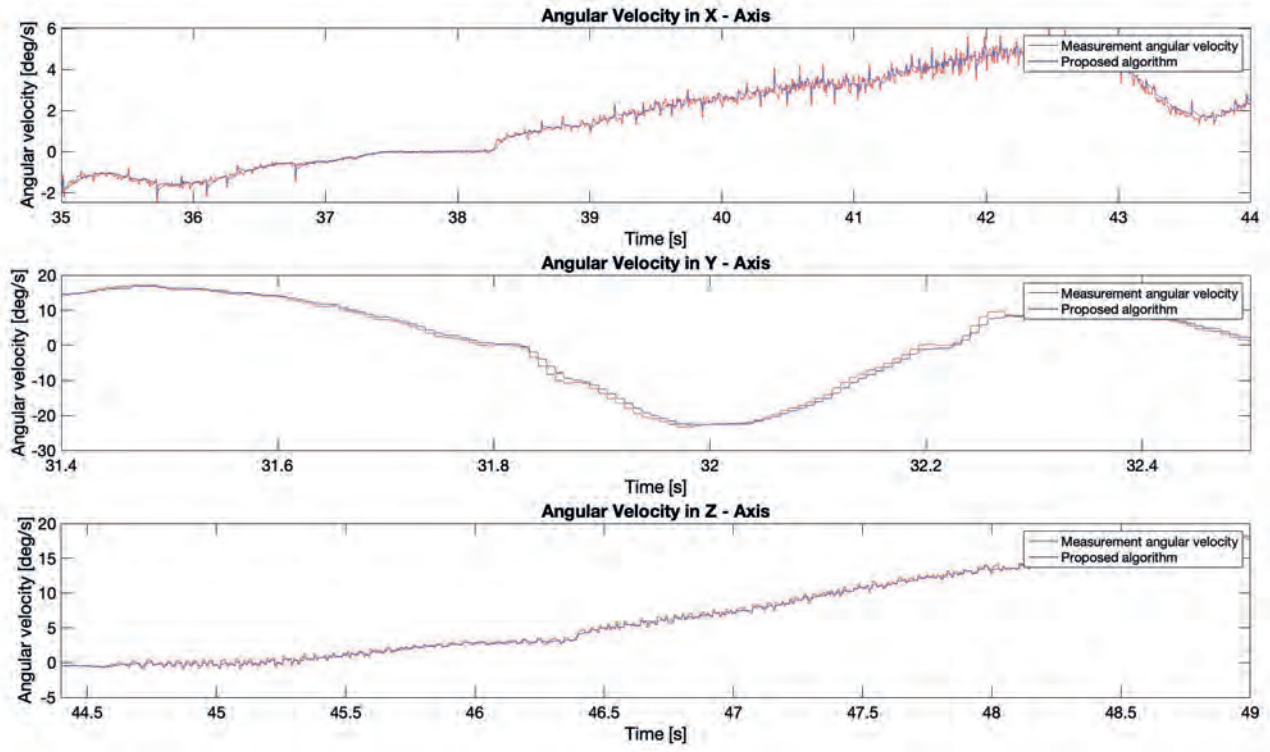

Fig. 3. Comparison of the measured angular velocity signals from gyroscopes with the filtered signals in the dynamic test
Rys. 3. Porównanie sygnałów zmierzonych prędkości kątowych z giroskopów z sygnałami przefiltrowanymi w badaniu dynamicznym

depending on the axis being analyzed. The algorithm performed best in reducing noise and improving measurement accuracy on the rocket's roll axis (X-axis). Delays in this axis were minimal, and the algorithm's match to actual angular velocity values was most precise, indicating the algorithm's effectiveness at relatively low angular velocity amplitudes in this channel. On the Y and Z axes, despite lower angular velocity amplitudes compared to the X-axis, larger delays were observed. This is likely due to the limited number of a coefficients, which should have had a greater number of discrete values in the process of scaling the Q matrix. It is also worth noting that the values were sampled at 125 Hz, which further limited the real-time effectiveness of the algorithm. The lower sampling frequency may have reduced the algorithm's ability to respond quickly to sudden changes in the rocket's dynamics, which was particularly evident on the Y and Z axes. Figures 4 and 6 show the variability of the Q-matrix gain coefficients over time, respectively for laboratory tests (Fig. 4)

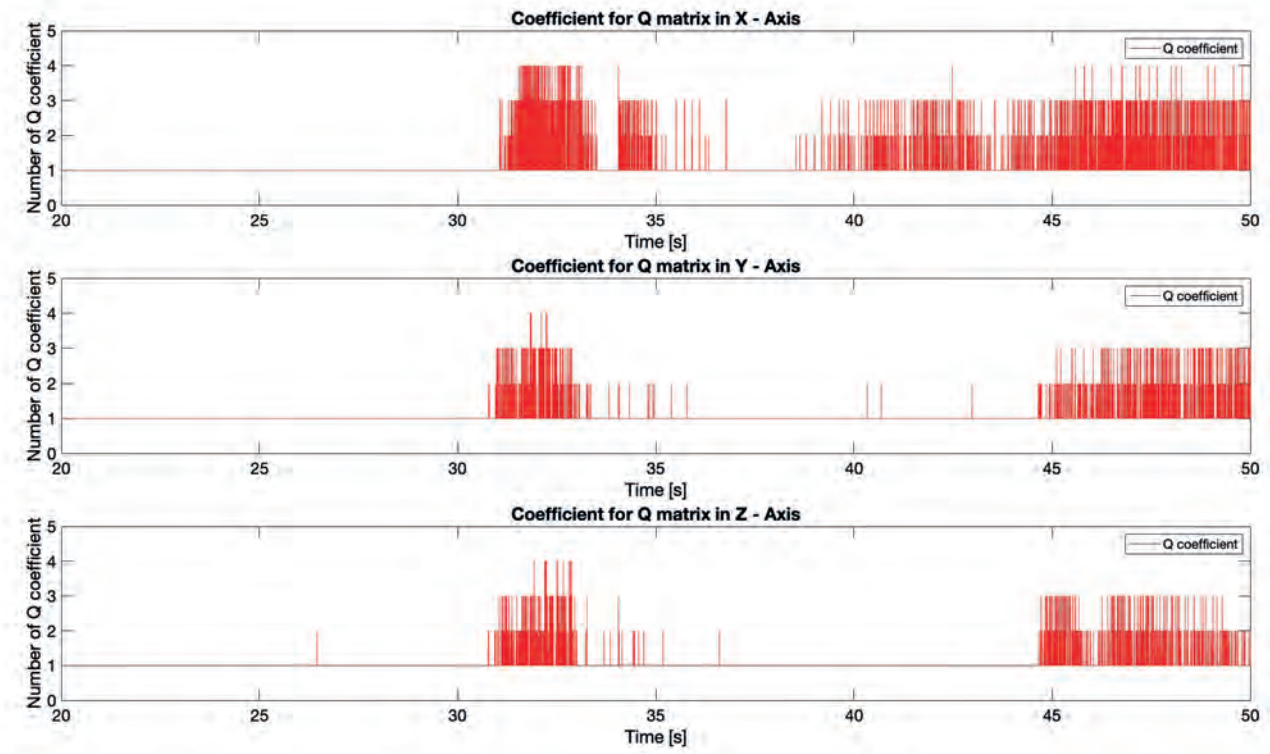

Fig. 4. The results of coefficients a scaling the matrix Q during dynamic test
Rys. 4. Przebieg wykorzystywanych współczynników skali do macierzy Q dla badania dynamicznego

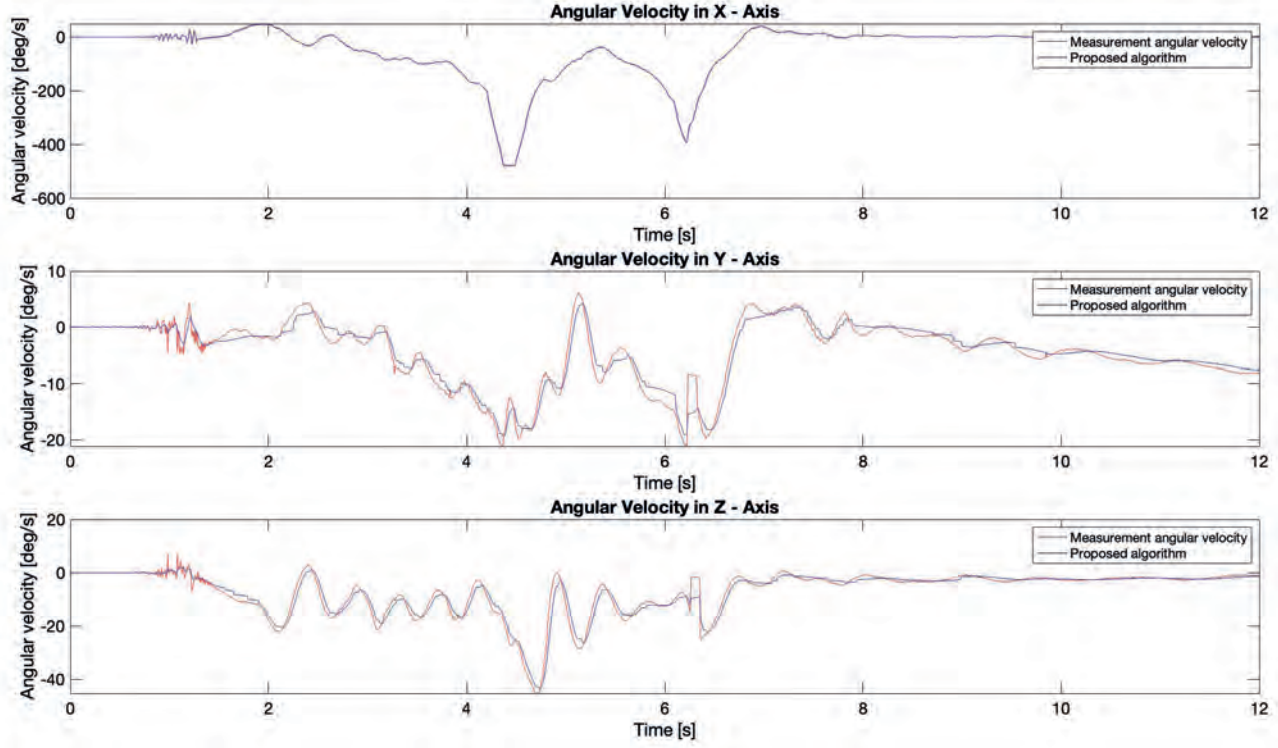

Fig. 5. Characteristics of changes in the measured angular velocity signals from gyroscopes and filtered signals during the guided rocket flight test
Rys. 5. Charakterystyka zmian sygnałów zmierzonych prędkości kątowych z giroskopów z sygnałami przefiltrowanymi w badaniu lotu rakiety sterowanej

and for the actual rocket flight (Fig. 6). The perpendicular axis represents the individual coefficient numbers from a_1 to a_4.

4. Discussion

Several key issues related to the Kalman filter algorithm, Q-matrix gain coefficients, and hardware limitations of the MEMS gyroscopes need to be discussed in detail.

Firstly, the Kalman filter algorithm in its current form uses a variable process noise covariance matrix Q, whose values are modified by coefficients dependent on the rocket's dynamics. These coefficients do not change continuously but are adjusted in discrete steps according to the current flight conditions, specifically based on the increments of angular velocity at a given moment in time.

The analysis of the results showed that the largest estimation errors and delays are associated with the coefficients a_2 and

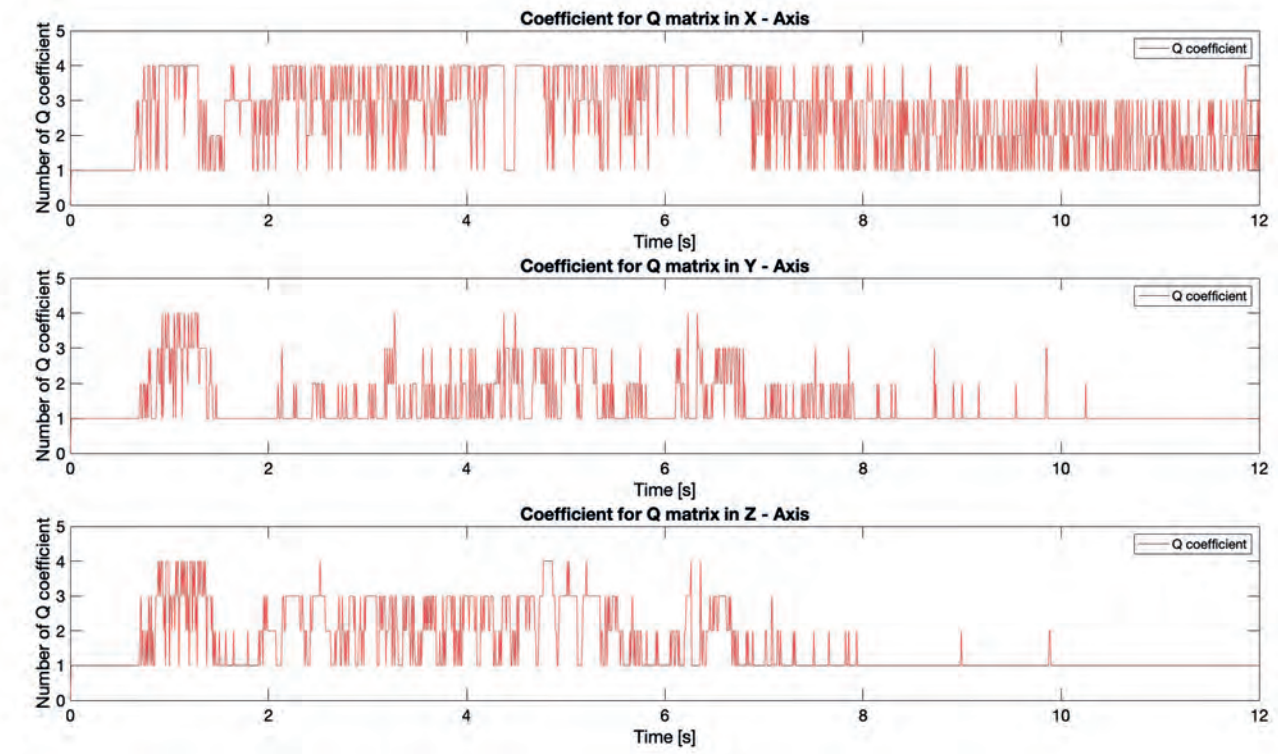

Fig. 6. The results of coefficients a scaling the matrix Q during missile flight test
Rys. 6. Charakterystyka zmian wykorzystywanych współczynników skali do macierzy Q podczas lotu rakiety sterowanej

a_3, particularly in the Y and Z axes. The available ranges of these coefficients proved insufficient, especially during intensive rocket maneuvers, where angular velocities change rapidly with large amplitudes. Increasing the number of available coefficient values within the ranges of a_2 and a_3 would enable the algorithm to more precisely adjust the parameters of the Q matrix to rapid changes in the flight dynamics. As a result, the response delays of the filter and state prediction errors would be reduced. Such a modification could significantly improve the estimation accuracy during dynamic rocket maneuvers, where precise determination of motion parameters is critical.

The current sampling frequency of 250 Hz and 125 Hz, although appropriate for many applications, proved to be insufficient in the context of high-dynamic rocket maneuvers. In the case of more complex movements, such as rapid rotations in the yaw, pitch, and roll channels, observed signal delays may be the result of too low a sampling frequency of the IMU. The author plans to increase the sampling frequency to at least 1 kHz, which will allow for a more accurate reflection of dynamic changes and better synchronization of the algorithm with the actual conditions of the rocket flight. Increasing the sampling frequency could not only reduce delays but also improve the quality of the data provided to the filtering algorithm, which will result in more precise state estimation.

Although the MEMS gyroscopes used in the research offer many advantages, such as low weight and cost, they also have their limitations, particularly in terms of measurement accuracy. For MEMS sensors, some errors, such as drift or inherent noise, are difficult to fully compensate for, especially in extreme dynamic conditions like rocket flight. It is worth noting that while the Kalman filter algorithm effectively reduces noise and compensates for systematic errors, complete compensation for all errors is impossible with MEMS sensors. However, in applications such as rocket guidance, the autopilot can handle small measurement errors, maintaining appropriate stabilization and precise guidance to a target point in space. This means that despite some limitations, the navigation system can operate at a satisfactory level for the planned mission execution.

In conclusion, the proposed changes to the algorithm and the increase in sampling frequency should significantly improve the accuracy and performance of the navigation system. Despite some hardware limitations, especially with MEMS gyroscopes, further modifications to the algorithm and optimization of operational parameters will allow for even better results in future studies.

References

1. Thienel J.K., Sanner R.M., *A Coupled Nonlinear Spacecraft Attitude Controller and Observer with an Unknown Constant Gyro Bias and Gyro Noise*, "IEEE Transactions on Automatic Control", Vol. 48, No. 11, 2003, 2011–2015, DOI: 10.1109/TAC.2003.819289.
2. Gelb A., Sutherland A., *Design approach for reducing gyro--induced errors in strapdown inertial systems*, Control and Flight Dynamics Conference, 1968, DOI: 10.2514/6.1968-830.
3. Miller J.E., Feldman J., *Gyro reliability in the Apollo Guidance, Navigation and Control system*, "Journal of Spacecraft and Rockets", Vol. 5, No. 6, 2008, 638–643, DOI: 10.2514/3.29323.
4. Mark J., Brown A., Matthews T., *Quantization reduction for evaluating laser gyro performance using a moving average filter*, IEEE International Conference on Acoustics, Speech and Signal Processing 1984, DOI: 10.1109/ICASSP.1984.1172629.
5. Zhu C., Cai S., Yang Y., Xu W., Shen H., Chu H., *A Combined Method for MEMS Gyroscope Error Compensation Using a Long Short-Term Memory Network and Kalman Filter in Random Vibration Environments*, "Sensors", Vol. 21, No. 4, 2021, DOI: 10.3390/s21041181.
6. Zhu Z., Bo Y., Jiang C., *A MEMS Gyroscope Noise Suppressing Method Using Neural Architecture Search Neural Network*, "Mathematical Problems in Engineering", 2019, DOI: 10.1155/2019/5491243.
7. Jiang C., Chen S., Chen Y., Zhang B., Feng Z., Zhou H., Bo Y., *A MEMS IMU De-Noising Method Using Long Short Term Memory Recurrent Neural Networks* (*LSTM--RNN*), "Sensors", Vol. 18, No. 10, 2018, DOI: 10.3390/s18103470.
8. Zhang H., Wang W., Li W., Wang P., Ren G., Ma G., Wang S., Zheng Yu., Shluga S.N., *An estimation of the mems gyroscope error based on the Kalman filter algorithm*, "Telecommunications and Radio Engineering", Vol. 78, No. 4, 2019, 1295–1301, DOI: 10.1615/TelecomRadEng.v78.i14.70.
9. Guo H., Hong H., *Research on Filtering Algorithm of MEMS Gyroscope Based on Information Fusion*, "Sensors", Vol. 19, No. 16, 2019, DOI: 10.3390/s19163552.
10. Liu Y., Guo Z., Zhang Q., *Modeling of MEMS gyroscope Random Error Based on Kalman Filter*, IEEE Symposium Series on Computational Intelligence (SSCI) 2019, DOI: 10.1109/SSCI44817.2019.9002682.
11. Chia J., Low K., Goh S., Xing Y., *A low complexity Kalman filter for improving MEMS based gyroscope performance*, Proceedings of the 2016 IEEE Aerospace Conference, DOI: 10.1109/AERO.2016.7500795.
12. Noureldin A., Karamat T.B., Georgy J., *Inertial Navigation System, Kalman Filter*, "Fundamentals of Inertial Navigation, Satellite-based Positioning and their Integration", Springer 2012, 125–166, 225–245, DOI: 10.1007/978-3-642-30466-8.
13. Xue L., Jang C., Chang H., Yang Y., Qin W., Yuan W., *A novel Kalman filter for combining outputs of MEMS gyroscope array*, "Measurement", Vol. 45, No. 4, 2012, 745–754, DOI: 10.1016/j.measurement.2011.12.016.
14. Erzberger H., *Application of Kalman Filtering to error correction of inertial navigators*, National Aeronautics and Space Administration, 1967.
15. Galante J.M., Sanner R.M., *A Nonlinear Adaptive Filter for Gyro Thermal Bias Error Cancellation*, AIAA Guidance, Navigation and Control Conference 2012, DOI: 10.2514/6.2012-4475.
16. Brown S.D., Rutan S.C., *Adaptive Kalman Filtering*, "Journal of Research of the National Bureau of Standards", Vol. 90, No 6, 1985, 403–407.
17. Fazelinia M., Ebadollahi S., Ganjefar S., *Stochastic analysis of drift error of gyroscope in the single-axis attitude determination*, "Measurement", Vol. 237, 2024, DOI: 10.1016/j.measurement.2024.115136.
18. Kim I., Kang T., Lee J.G., *Design of a gyroscope with minimum error covariance*, "Control Engineering Practice", Vol. 3, No. 7, 1995, 933–937, DOI: 10.1016/0967-0661(95)00076-7.
19. Hameed Aslam Q., Iqbal A., Bibi F., Bibi S., *Error Estimation of Inertial Sensors using Allan Variance*, "IFAC Proceedings Volumes", Vol. 41, No. 1, 2008, 167–171, DOI: 10.3182/20080408-3-IE-4914.00030.
20. *Allan Variance: Noise Analysis for Gyroscopes*, Freescale Semiconductor, Application Note 2015, Document Number: AN5087.
21. Hou H., *Modeling Inertial Sensors Using Allan Variance*, Master Degree, University of Calgary 2004.
22. Kadian K., Garhwal S., Kumar A., *Quantum walk and its application domains: A systematic review*, "Computer Science Review", Vol. 41, 2021, DOI: 10.1016/j.cosrev.2021.100419.

23. Boncelet C., Chapter 7 – *Image Noise Models*, "The Essential Guide to Image Processing", 2009, 143–167, DOI: 10.1016/B978-0-12-374457-9.00007-X.
24. Zeng Y., Liu Y., Zhang M., *A method for compensating random errors in MEMS gyroscopes based on interval empirical mode decomposition and ARMA*, "Measurement Science and Technology", Vol. 35, No. 1, 2023, DOI: 10.1088/1361-6501/ad00d3.
25. Wang J., Yang G., Liu F., *An InRun Automatic Demodulation Phase Error Compensation Method for MEMS Gyroscope in Full Temperature Range*, "Micromachines", Vol. 15, No. 7, 2024, DOI: 10.3390/mi15070825.
26. Sheng Cai., Zhu C., Yang Y., *A Combined Method for MEMS Gyroscope Error Compensation Using a Long Short-Term Memory Network and Kalman Filter in Random Vibration Environments*, "Sensors", Vol. 21, No. 4, 2021, DOI: 10.3390/s21041181.
27. Long Y., Liu Z., Hao C., *MEMS Gyroscope Multi-Feature Calibration Using Machine Learning Technique*, arXiv, 2024, DOI: 10.48550/arXiv.2410.07519.
28. Pan F., Zheng S., Yin Ch., *MoE-Gyro: Self-Supervised Over-Range Reconstruction and Denoising for MEMS Gyroscopes*, arXiv, 2024, DOI: 10.48550/arXiv.2506.06318.
29. Randall R.B., Tordon M.J., *Data Acquisition,* "Encyclopedia of Vibration", 2001, 364-376, DOI: 10.1006/rwvb.2001.0142.
30. Mohammadi Z., Salarieh H., *Investigating the effects of quadrature error in parametrically and harmonically excited MEMS rate gyroscopes*, "Measurement", Vol. 87, 2016, 152–175, 10.1016/j.measurement.2016.03.013.
31. Brisebois G., *Op Amp Selection Guide for Optimum Noise Performance*. Chapter 422, Analog Circuit Design 2015, Vol. 3, 907–908.

Other sources

32. Extended Kalman Filter, https://en.wikipedia.org/wiki/Extended_Kalman_filter.
33. Random Walk, https://en.wikipedia.org/wiki/Random_walk.
34. Quantization (signal processing), https://en.wikipedia.org/wiki/Quantization_(signal_processing).
35. Quantization Noise, https://classes.engineering.wustl.edu/ese488/Lectures/Lecture5a_QNoise.pdf.

Identyfikacja i kompensacja błędów pomiarowych giroskopów: filtracja sygnałów na podstawie badań statycznych i dynamicznych inercyjnego systemu nawigacji

Streszczenie: Celem pracy była analiza identyfikacji błędów pomiarowych w giroskopach typu MEMS, które stanowią główne źródło danych dla bezwładnościowego systemu nawigacyjnego (INS) opracowanej rakiety. Badania skupiły się na analizie błędów przeprowadzając testy statyczne i dynamiczne, po których nastąpiła szczegółowa analiza danych pomiarowych prędkości kątowej również z lotu rakiety kierowanej do określonego punktu w przestrzeni. Celem badania było określenie i filtrowanie błędów pomiarowych giroskopu, takich jak bias, random walk i szum. Na podstawie wyników zaproponowano filtr adaptacyjny, który dostosowuje się do zmieniającej się dynamiki rakiety, umożliwiając skuteczniejszą kompensację tych błędów. W części końcowej przedstawiono wnioski, które zidentyfikowały niedociągnięcia w algorytmie i nakreśliły kierunki dalszych prac nad jego optymalizacją. Algorytm został zweryfikowany w warunkach statycznych, dynamicznych i rzeczywistych warunków lotu rakiety.

Słowa kluczowe: korekta błędów pomiarowych, żyroskopy MEMS, filtry adaptacyjne, nawigacja inercyjna, systemy nawigacji rakiet

Szymon Elert, MSc Eng.
elerts@witu.mil.pl
ORCID: 0000-0003-2491-650X

Szymon Elert received his MSc degree in Military University of Technology in Warsaw in 2017. From the start of his career, he has been closely involved in rocket technology and the design of GNC systems. He is actively engaged in multiple projects, developing software for rockets, designing algorithms and preparing mathematical simulations.